An Iterative FEM for Scattering by a 3-D Cavity-Backed Aperture

Jongkuk Park, *Student Member, IEEE*, Jungwon Lee, *Student Member, IEEE*, Heeduck Chae, *Student Member, IEEE*, and Sangwook Nam, *Member, IEEE*

***Abstract*—A finite-element method (FEM)-based hybrid method (or iterative FEM) is successfully applied to a three-dimensional (3-D) scattering problem without the effect of internal resonance. With only a small number of meshes around a 3-D scatterer, this FEM is shown to give an accurate result through several iterative updates of the boundary conditions. To confirm the efficiency of this method, scattering from a 3-D cavity-backed aperture is analyzed and the results obtained are compared with the same obtained by another conventional method.**

***Index Terms*—Internal resonance, iterative FEM, radiation-type boundary condition.**

I. Introduction

THE finite-element method (FEM) has been widely used as a powerful tool for solving bounded problems. However, for open-region problems, since the mesh of the computational domain cannot be extended to infinity, an appropriate boundary condition must be applied or special action must be taken in order to simulate the effect of the infinite domain. As known widely, in order to apply the FEM to radiation and scattering problems, a number of techniques have been proposed by many researchers. Among these techniques, the hybrid methods such as the finite-element boundary integral method (FEBIM) and the methods incorporating various kinds of absorbing boundary conditions (ABCs) and perfectly matched layers (PMLs) have been used by many [1], [2] since they are robust and give good results. However, each method has its inherent shortcomings and, thus, many efforts have been made to improve its efficiency.

As another approach of these attempts, the FEM-based iteration method (or iterative FEM) has been proposed before [3]–[7]. According to this approach, the FEM was shown to give an accurate result efficiently with only a small number of meshes around a scatterer through several times of iterative updates of the boundary conditions. The proposed method has been applied to two-dimensional electrostatic and scattering problems [3]–[5] and then extended to three-dimensional (3-D) scattering problems [6] and 3-D guided-wave problems [7]. However, this method has been found not to be suitable for characterizing the scattering by an object such as a cavity or a scatterer with a resonant size since the Dirichlet boundary condition used in this method causes internal resonance [8] to occur, and this internal resonance unfortunately corrupts a true solution. To alleviate this problem, the iterative FEM in conjunction with a radiation-type boundary condition [9] has been suggested and applied to a two-dimensional scattering problem successfully without internal resonance.

Manuscript received February 17, 2001. This work was supported under the Brain Korea 21 Project.

The authors are with the Applied Electromagnetics Laboratory, School of Electrical Engineering, Seoul National University, Seoul 151-742, Korea (e-mail: pjk@inmac3.snu.ac.kr).

Publisher Item Identifier S 0018-9480(01)09378-4.

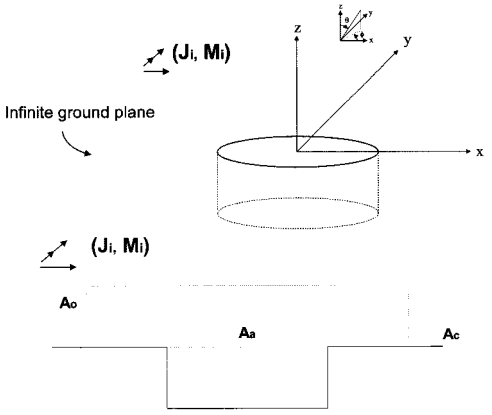

Fig. 1. Geometry of a cavity-backed aperture in a ground plane.

In this paper, the above iterative FEM with a radiation-type boundary condition is extended to involve a 3-D vector-wave equation and applied to scattering from a 3-D cavity-backed aperture as a simple example. To verify accuracy and efficiency of the result, this method is compared with the conventional FEBIM.

II. Formulation

Consider a 3-D cavity-backed aperture in a ground plane, as illustrated in Fig. 1, where A_c is a perfect conducting boundary surface and A_o is a fictitious boundary surface on which the finite-element meshes are terminated. According to the conventional iterative FEM, the tangential electric field is determined and updated on this fictitious surface A_o as the Dirichlet boundary condition. However, the FEM solution obtained from this tangential electric field on A_o is found to be corrupted by the modal solution of an imaginary cavity bounded by A_c and A_o. Thus, a radiation-type boundary condition should be applied on this fictitious surface A_o in order to avoid this internal resonance.

In general, the Sommerfeld radiation condition is given by

$$\hat{n} \times \nabla \times \mathbf{E_s} + jk_0 \hat{n} \times \hat{n} \times \mathbf{E_s} = \mathbf{0} \tag{1}$$

where k_0 is the free-space wavenumber, $\mathbf{E_s}$ is the scattered electric field, and $\hat{n}$ is a unit vector normal to the fictitious surface A_o if it is placed in the far-field region. However, since the fictitious surface A_o should be placed considerably close to the scattering surface A_a, the Sommerfeld radiation condition in the far-field region is not suitable for this case and should be reconstructed as

$$\hat{n} \times \nabla \times \mathbf{E_s} + jk_0 \hat{n} \times \hat{n} \times \mathbf{E_s} = \mathbf{U_s}. \tag{2}$$

This radiation boundary condition means that the left-hand side of the Sommerfeld radiation condition does not vanish in the near-field region. The key idea is based on updating this residual term $\mathbf{U_s}$. For the formulation in terms of the total field, (2) is rewritten as

$$\hat{n} \times \nabla \times \mathbf{E} + jk_0 \hat{n} \times \hat{n} \times \mathbf{E} = \mathbf{U} \tag{3}$$

where $\mathbf{E}$ is the total electric field and $\mathbf{U}$ is the sum of $\mathbf{U_s}$ and the residual term due to the incident field.

With this boundary condition, the functional is given by

$$F(\mathbf{E}) = \frac{1}{2} \iiint_V \frac{1}{\mu_r} (\nabla \times \mathbf{E}) \cdot (\nabla \times \mathbf{E}) - k_0^2 \epsilon_r \mathbf{E} \cdot \mathbf{E} dv + \frac{jk_0}{2} \iint_{A_o} (\hat{n} \times \mathbf{E}) \cdot (\hat{n} \times \mathbf{E}) ds + \iint_{A_o} \mathbf{E} \cdot \mathbf{U} ds \tag{4}$$

where μ_r and ϵ_r are the relative permeability and relative permittivity, respectively, V denotes the volume of the imaginary cavity bounded by A_c and A_o, and A_o denotes the fictitious boundary surface on which the meshes are terminated. If the value of $\mathbf{U}$ is known exactly, the exact value of the electric field everywhere can be calculated by seeking the stationary point of the given functional. However, the residual vector $\mathbf{U}$, as well as the electric field $\mathbf{E}$ is unknown and, thus, the value of the vector $\mathbf{U}$ is approximated initially on the assumption that the electric field $\mathbf{E}$ in (3) is the same as an incident electric field. By discretizing the volume V into small vector finite elements [1] and taking the partial derivatives of F in (4), we obtain the following set of linear algebraic equations [1]:

$$\mathbf{A}\mathbf{x}^{(0)} = \mathbf{b}^{(0)} \tag{5}$$

where $\mathbf{A}$ is a square matrix depending on the geometry and dielectric materials, $\mathbf{x}^{(0)}$ is a vector representing the unknown electric field including that on the boundary surface A_o, $\mathbf{b}^{(0)}$ is a source vector calculated from the value of the residual vector $\mathbf{U}$, and superscript (0) denotes the zeroth iteration. As mentioned above, the solution vector given by (5) is not exact since $\mathbf{U}$ includes only the effect of the incident field. In order to update the value of $\mathbf{U}$ on A_o, we introduce the following equivalent magnetic current $\mathbf{M}$ on the aperture surface A_a in accordance with the equivalence principle [10]:

$$\mathbf{M} = \mathbf{E_a} \times \hat{n} \tag{6}$$

where $\mathbf{E_a}$ is the electric field on the aperture, which is calculated in (5), and $\hat{n}$ is a unit vector normal to the aperture surface. In order to calculate the scattered field generated by this equivalent magnetic current source, we invoke image theory [10]. Thus, the total fields on the boundary surface A_o are the sum of this scattered field, the incident field, and the field reflected by a perfect electric conductor (PEC) ground plane. The incident and reflected fields are invariant with iterations and, thus, only the scattered field is updated on each iteration. In order to describe this relationship mathematically, we define a vector $\mathbf{P}$ as

$$\mathbf{P} \equiv \nabla \times \mathbf{E} + jk_0 \hat{n} \times \mathbf{E} \tag{7}$$

for convenience. From the simple relation of $\mathbf{U} = \hat{n} \times \mathbf{P}$, $\mathbf{U}$ is rewritten as

$$\mathbf{U} = \hat{n} \times \mathbf{P_{ir}} + \hat{n} \times \mathbf{P_s} \tag{8}$$

where $\mathbf{P_{ir}}$ is calculated with the incident and reflected electric fields and $\mathbf{P_s}$ is calculated with the scattered electric field. The last term of the functional then becomes

$$\iint_{A_o} \mathbf{E} \cdot \mathbf{U} ds = -\iint_{A_o} (\hat{n} \times \mathbf{E}) \cdot \mathbf{P_{ir}} ds - \iint_{A_o} (\hat{n} \times \mathbf{E}) \cdot \mathbf{P_s} ds. \tag{9}$$

The excitation is assumed to be a plane wave given by

$$\mathbf{E}^i(\mathbf{r}) = \left\{ \left(\hat{\alpha} \cdot \hat{\theta}^i \right) \hat{\theta}^i + \left(\hat{\alpha} \cdot \hat{\phi}^i \right) \hat{\phi}^i \right\} e^{-j\mathbf{k}^i \cdot \mathbf{r}} \tag{10}$$

where $\hat{\alpha} = \hat{\theta}^i \cos\alpha + \hat{\phi}^i \sin\alpha$ is the polarization vector, $\mathbf{k}^i$ is the propagation vector given by

$$\mathbf{k}^i = -k_0 \left(\sin\theta^i \cos\phi^i \hat{\mathbf{x}} + \sin\theta^i \sin\phi^i \hat{\mathbf{y}} + \cos\theta^i \hat{\mathbf{z}} \right) \tag{11}$$

where $\hat{\theta}^i$, $\hat{\phi}^i$ are the unit vectors in the spherical system and associated with the incident angles θ^i and ϕ^i, respectively. With this incident field, we can calculate the reflected field easily so that the vector $\mathbf{P_{ir}}$ is obtained straightforwardly from (7). Next, in order to calculate the vector $\mathbf{P_s}$ due to the equivalent magnetic current (6), we introduce the vector potential $\mathbf{F}$ [10]. With this vector potential $\mathbf{F}$, $\mathbf{P_s}$ is given by

$$\mathbf{P_s} = \nabla \times \mathbf{E_s} + jk_0 \hat{n} \times \mathbf{E_s} = -\left\{ k_0^2 \mathbf{F} + \nabla(\nabla \cdot \mathbf{F}) \right\} - jk_0 \hat{n} \times (\nabla \times \mathbf{F}) \tag{12}$$

where $\hat{n}$ is a unit vector normal to the artificial boundary surface A_o and $\mathbf{E_s}$ is the scattered electric field. The vector potential $\mathbf{F}$ is given by

$$\mathbf{F} = \iint_{A_a} 2\mathbf{M}(\mathbf{r}') G_0(\mathbf{r}, \mathbf{r}') ds' \tag{13}$$

where $\mathbf{M}(\mathbf{r}')$ denotes the equivalent magnetic current over the aperture A_a and $G_0(\mathbf{r}, \mathbf{r}')$ denotes the free-space Green's function given by

$$G_0(\mathbf{r}, \mathbf{r}') = \frac{e^{-jk_0|\mathbf{r}-\mathbf{r}'|}}{4\pi|\mathbf{r}-\mathbf{r}'|} \tag{14}$$

where $\mathbf{r}$ and $\mathbf{r}'$ are the position vectors that denote the observation and source points, respectively. Substituting (13) into (12) and manipulating the vector equation, we obtain

$$\mathbf{P_s} = -2\left(k_0^2 \iint_{A_a} \mathbf{M} G_0 ds' + \iint_{A_a} (\nabla' \cdot \mathbf{M}) \nabla G_0 ds'\right) + 2jk_0 \hat{n} \times \left(\iint_{A_a} \mathbf{M} \times \nabla G_0 ds'\right). \quad (15)$$

By the typical finite-element procedure, the cavity aperture, as well as the volume, is subdivided into small surface patches, and (9) is then written as the following matrix equation:

$$\mathbf{b_o}^{(1)} = \mathbf{b_{o,ir}} + \mathbf{Q}\mathbf{x_a}^{(0)}. \quad (16)$$

where $\mathbf{b_o}^{(1)}$ is the source vector to be used at the next iteration, $\mathbf{b_{o,ir}}$ is the source vector invariant with iterations, which is calculated with the incident and reflected fields, $\mathbf{x_a}^{(0)}$ is the electric-field coefficient vector on the aperture calculated at the zeroth iteration, and $\mathbf{Q}$ is the rectangular matrix that correlates the electric-field coefficients with the source vector. Note that a subscript "$\mathbf{o}$" denotes a vector composed of only the values at the edges on the artificial boundary A_o and "$\mathbf{a}$" denotes a vector composed of only the values at the edges on the aperture A_a. Thus, $\mathbf{Q}$ is an N_o by N_a matrix where N_o and N_a are the numbers of edges placed on A_o and A_a, respectively.

Equations (5) and (16) are generalized to the mth iteration and written as

$$\begin{aligned} \mathbf{A}\mathbf{x}^{(\mathrm{m})} &= \mathbf{b}^{(\mathrm{m})} \\ \mathbf{b_o}^{(\mathrm{m}+1)} &= \mathbf{b_{o,ir}} + \mathbf{Q}\mathbf{x_a}^{(\mathrm{m})}. \end{aligned} \quad (17)$$

This iteration procedure can be made computationally efficient if the following properties are fully exploited in the implementation. First, matrices $\mathbf{A}$ and $\mathbf{Q}$ are invariant during the iterations so that they are computed only once at the initial state of the procedure. Second, since the system matrix $\mathbf{A}$ is generated by a standard finite-element procedure and, thus, it is symmetric and highly sparse, it is solved efficiently by means of a standard finite-element solver. If a direct solver is used, the decomposition of $\mathbf{A}$, which is time consuming, is performed only once at the zeroth iteration. If an iterative solver is used, the solution at the mth iteration is a good initial guess for the iterative solver at the $(\mathrm{m}+1)$th iteration, and the preconditioner, if any, is calculated only once. Third, only a very small increase of the computational domain is necessary since the fictitious boundary surface can be placed so close around the scattering objects. These features make the iterative FEM competitive with other techniques as far as computing time and memory requirements are concerned. In addition, preexisting FEM codes for bounded problems may be easily incorporated into this iteration procedure and only one part has to be added that corresponds to the computation of the matrix $\mathbf{Q}$. Note that singularity extraction, which should be carried out in the FEBIM, is not necessary in this calculation since the fictitious boundary surface is placed at a given distance from the aperture surface.

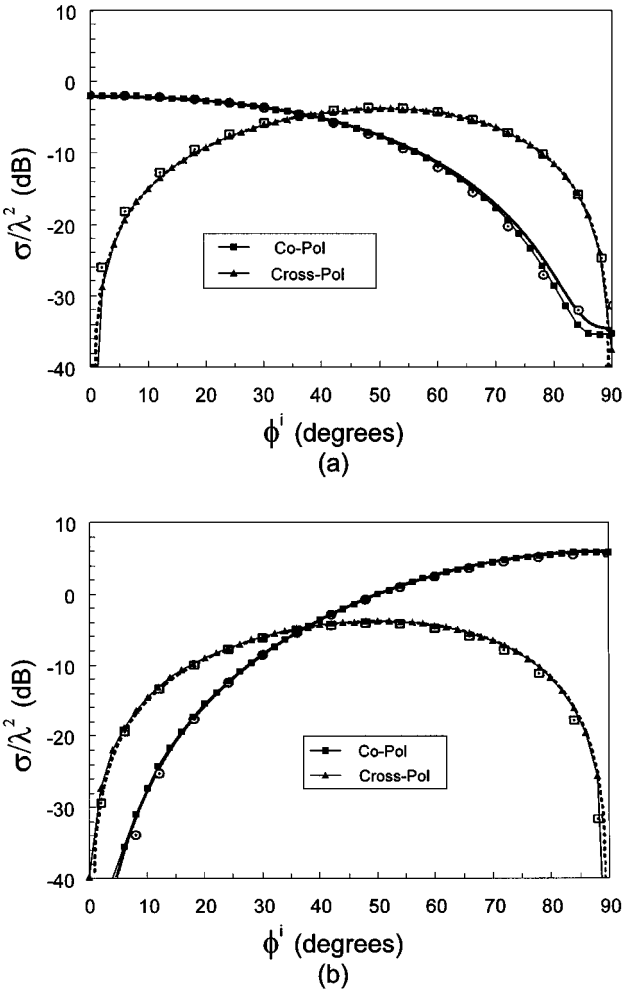

Fig. 2. Monostatic *RCS* patterns for a deep empty rectangular cavity of dimensions $0.7\lambda \times 0.1\lambda \times 1.73\lambda$ versus incidence angle ϕ^i when $\theta^i = 40°$. Solid lines with filled squares and triangles represent this method; solid and dotted lines represent the FEBIM and vacant circles and squares represent the moment method/modal approach. (a) $\alpha = 90° \left(\mathbf{E} = \hat{\phi} E_\phi\right)$. (b) $\alpha = 0° \left(\mathbf{E} = \hat{\theta} E_\theta\right)$.

III. Numerical Results

In order to examine the validity and the capability of the iterative FEM, we have analyzed various shapes of cavity-backed apertures in a ground plane. In this study, triangular prism edge-based elements [11] are used to be able to deal with an arbitrary cross section of a cavity, as well as a rectangular cavity and, thus, the aperture of the cavity is divided into triangular patches.

First, with the excitation by a plane wave, scattering from a deep empty rectangular cavity of dimensions $0.7\lambda \times 0.1\lambda \times 1.73\lambda$ is considered and its results are illustrated in Fig. 2. The co-polarized and cross-polarized monostatic *RCS* patterns of the cavity versus incidence angle ϕ^i when $\theta^i = 40°$ are compared with data obtained by the FEBIM [12] and the moment method/modal approach [13]. Good agreement is shown between the results.

Fig. 3 shows the convergence characteristics with respect to the distance between the artificial boundary surface A_o and the

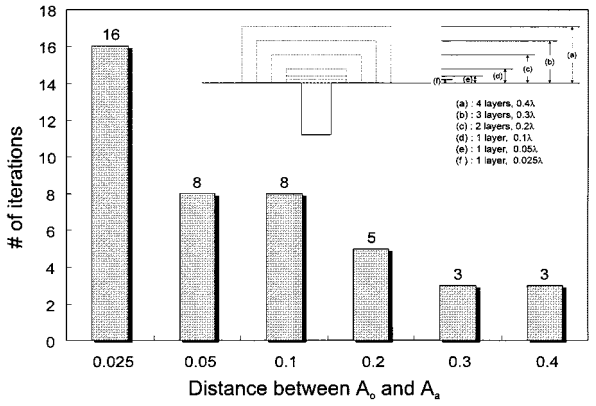

Fig. 3. Convergence characteristics according to the position of the artificial boundary surface.

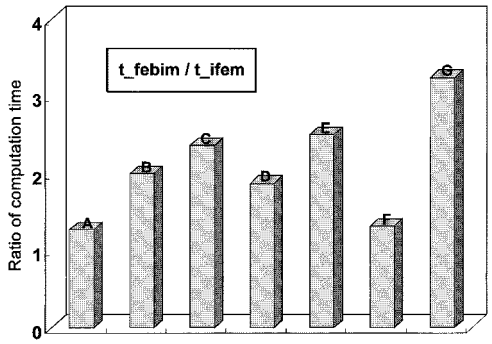

Fig. 4. Computational efficiency (computation time): iterative FEM versus FEBIM. A: $1.5\lambda \times 0.05\lambda \times 0.25\lambda$ narrow rectangular crack. B: $0.5\lambda \times 0.5\lambda \times 0.3\lambda$ shallow square cavity. C: $0.5\lambda \times 0.5\lambda \times 1.75\lambda$ deep square cavity. D: $1.0\lambda \times 1.0\lambda \times 1.0\lambda$ large square cavity. E: Radius: 0.25λ depth: 0.3λ shallow circular cavity. F: Radius: 0.5λ depth: 1.5λ deep circular cavity. G: Radius: 1.0λ depth: 0.3λ large circular cavity.

aperture surface A_a. As expected, the number of iterations increases as the artificial surface A_o is getting closer to the aperture surface A_a. On the contrary, if A_o is placed too far from A_a in order to reduce the number of iterations, however, the number of meshes increases rapidly and, thus, the overall computation time and memory requirement increase as well. Therefore, the optimal criterion should be determined. Unfortunately, since the convergence condition depends on the distance between A_o and A_a and the whole FE discretization in a very complex manner, it is very difficult to propose an analytical criterion. Thus, we have empirically determined the almost optimal distance between the two surfaces through numerical experiments for numerous cavities with various shapes and sizes. Up to a size of 2λ of the aperture in a cavity, a distance of $0.1\lambda - 0.2\lambda$ between A_o and A_a is found to be enough for a solution to converge within only several times of iterations and this distance corresponds to one or two layer meshes of triangular prism elements.

With this criterion, the computation time taken by the iterative FEM is compared with that by the conventional FEBIM using a biconjugate gradient method. Fig. 4 shows the computational efficiency of the iterative FEM. For a fair comparison between the two methods, the number of elements only in the cavity is the same in both methods and, thus, the dimension of the system matrix of the iterative FEM is larger than that of the FEBIM. In

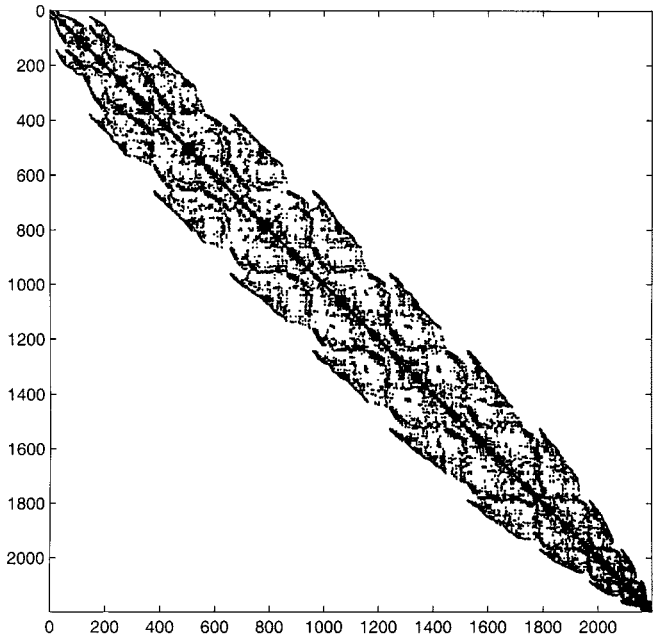

Fig. 5. Reduced bandwidth of the system matrix after Gibbs–Poole–Stockmeyer bandwidth profile reduction algorithm.

order to decompose this system matrix of the iterative FEM efficiently, at first we used the standard Gibbs–Poole–Stockmeyer bandwidth profile reduction algorithm [14] for the system matrix to be a banded form, as illustrated in Fig. 5 and a banded matrix $\mathrm{LDL^T}$ solver with the profile storage [1]. However, it is found that the reduced bandwidth is over several hundred, and this value is much larger than the maximum number of nonzero elements in a row of the system matrix, which is about 30 or less when triangular prism elements are used. This leaves much to be improved although the bandwidth reduction and the $\mathrm{LDL^T}$ decomposition considerably save both storage and operation count in the triangular factorization process. Thus, we have replaced the above with sparse matrix LU decomposition algorithm using minimum degree ordering [15], which is commonly used for reducing fill-in during factorization of a sparse matrix. With this algorithm, the iterative FEM is about twice or three times faster than the conventional FEBIM for scattering by various cavities, as shown in Fig. 4.

IV. Conclusions

An efficient iterative FEM in two dimensions, which avoids internal resonance, is extended to three dimensions and applied to scattering from a 3-D cavity-backed aperture. Through exhaustive numerical experiments, an empirical convergence criterion for this method is proposed. The validity and efficiency of this method is shown by comparing this method with the conventional FEBIM.

References

[1] J. M. Jin, *The Finite Element Method in Electromagnetics*. New York: Wiley, 1993.

[2] J. L. Volakis, A. Chatterjee, and L. C. Kempel, *Finite Element Method for Electromagnetics: Antennas, Microwave Circuits, and Scattering Applications*. Piscataway, NJ: IEEE Press, 1998.

[3] T. Roy, T. K. Sarkar, A. R. Djordjevic, and M. Salazar, "A hybrid method for terminating the finite element mesh (electrostatic case)," *Microwave Opt. Technol. Lett.*, vol. 8, no. 6, pp. 282–287, Apr. 1995.
[4] ——, "A hybrid method solution of scattering by conducting cylinders (TM case)," *IEEE Trans. Microwave Theory Tech.*, vol. 44, pp. 2145–2151, Dec. 1996.
[5] F. Xiao and H. Yabe, "Solution of scattering from conducting cylinders using an iterative method," *IEEE Trans. Magn.*, vol. 36, pp. 884–887, July 2000.
[6] M. Salazar, T. K. Sarkar, L. Garcia, T. Roy, and A. R. Djordjevic, *Iterative and Self-Adaptive Finite-Elements in Electromagnetic Modeling*. Norwood, MA: Artech House, 1998.
[7] J. Park, H. Chae, and S. Nam, "Efficient hybrid method for characterization of arbitrary-shaped discontinuities in rectangular waveguide," *Electron. Lett.*, vol. 35, no. 14, pp. 1170–1172, July 1999.
[8] A. F. Peterson, "The 'interior resonance' problem associated with surface integral equations of electromagnetics: Numerical consequences and a survey of remedies," *Electromagnetics*, vol. 10, no. 3, pp. 293–312, July–Sept. 1990.
[9] S. Alfonzetti, G. Borzi, and N. Salerno, "Iteratively-improved robin boundary conditions for the finite element solution of scattering problems in unbounded domains," *Int. J. Numer. Methods Eng.*, vol. 42, pp. 601–629, 1998.
[10] C. A. Balanis, *Advanced Engineering Electromagnetics*. New York: Wiley, 1989.
[11] J. Park and S. Nam, "Analysis of arbitrary shaped cross-sectional discontinuity in rectangular waveguides using FEM–BIM with triangular prism elements," in *Proc. IEEE AP-S Int. Symp. Dig.*, Montréal, QC, Canada, July 1997, pp. 672–675.
[12] J. M. Jin and J. L. Volakis, "A finite element-boundary integral formulation for scattering by three-dimensional cavity-backed apertures," *IEEE Trans. Antennas Propagat.*, vol. 39, pp. 97–104, Jan. 1991.
[13] K. Barkeshli and J. L. Volakis, "Electromagnetic scattering from an aperture formed by a rectangular cavity recessed in a ground plane," *J. Electromag. Waves Applicat.*, vol. 5, no. 7, pp. 715–734, 1991.
[14] N. E. Gibbs, W. G. Poole, Jr, and P. K. Stockmeyer, "An algorithm for reducing the bandwidth and profile of a sparse matrix," *SIAM J. Numer. Anal.*, vol. 13, no. 2, pp. 236–250, Apr. 1976.
[15] *SuperLU User's Guide*, [Online]. Available: http://www.netlib.org, 1999.

Jongkuk Park (S'97) was born in Seoul, Korea, in 1971. He received the B.S. and M.S. degrees in electronics engineering from the Seoul National University, Seoul, Korea, in 1995 and 1997, respectively, and is currently working toward the Ph.D. degree at the Seoul National University.

His research interests include numerical analysis and antenna and passive circuit design.

Jungwon Lee (S'01) was born in Seoul, Korea, in 1975. He received the B.S. and M.S. degrees in electrical engineering from the Seoul National University, Seoul, Korea, in 1998 and 2000, respectively, and is currently working toward the Ph.D. degree at the Seoul National University.

His research interests include computational electromagnetics and antenna and passive circuit design.

Heeduck Chae (S'01) was born in Daegu, Korea, in 1976. He received the B.S. and M.S. degrees in electrical engineering from the Seoul National University, Seoul, Korea, in 1999 and 2001, respectively, and is currently working toward the Ph.D. degree at the Seoul National University.

His research interests include array antennas and antenna measurement.

Sangwook Nam (S'87–M'88) received the B.S. degree from the Seoul National University, Seoul, Korea, in 1981, the M.S. degree from the Korea Advanced Institute of Science and Technology, Seoul, Korea, in 1983, and the Ph.D. degree from The University of Texas at Austin, in 1989, all in electrical engineering.

From 1983 to 1986, he was a Researcher at the Gold Star Central Research Laboratory, Seoul, Korea. Since 1990, he has been with Seoul National University, where he is currently a Professor in the School of Electrical Engineering. His research interests include analysis/design of electromagnetic (EM) structures, antennas, and microwave active/passive circuits.